NUMERICAL INVESTIGATION OF THE MOTION CHARACTERISTICS OF CYLINDRICAL FLOATING BODY IN WAVES USING THE VOLUME OF FLUID METHOD

(Reference No: IJME676, DOI No: 10.5750/ijme.v163iA3.801)

X Song and **W Liu**, Wuhan University of Technology, China, and T Xia, HiRain Technologies, China

KEY DATES: Submitted: 04/10/20; Final acceptance: 17/08/21; Published 16/11/21

SUMMARY

In this paper, a numerical hydrodynamic performance assessment of a full scale cylindrical floating body with different damping devices is presented. The motion characteristics of the full scale cylindrical floating body are investigated in regular and irregular wave conditions with different wave heights and periods. A numerical wave tank based on the two-phase Volume of Fluid (VOF) model was established. Approaches to the computational domain and overset-grids were investigated and were found to be suitable. Grid convergence was undertaken for the simulations. The numerical wave tank was performed to analyse the motion characteristics of the cylindrical floating body with arbitrary devices under different wave conditions by using the VOF method with an overset-grid technique. The motion characteristics of the cylindrical floating body with different damping devices were numerically investigated to provide more information on the effect of damping devices on the hydrodynamic performance. The conclusions of this paper give guidance in the motion characteristics and the damping device prototype design to be adopted under the specified wave conditions.

NOMENCLATURE

[Symbol]	[Definition] [(unit)]
f	Frequency (s^{-1})
f_P	Wave frequency at the spectral peak (s^{-1})
h	Water depth (m)
H	Wave height (m)
$H_{1/3}$	Significant wave height (m)
k	Wave number (m^{-1})
P	Pressure (N m^{-2})
$T_{1/3}$	Significant wave period (s)
T_P	Wave period at the spectral peak (s)
γ	Peak enhancement factor
μ_{air}	Molecule viscosity coefficient of air (N s m^{-2})
μ_t	Turbulent viscosity coefficient (N s m^{-2})
μ_{water}	Molecule viscosity coefficient of water (N s m^{-2})
υ	Kinematic viscosity (N s m^{-2})
ρ	Density of water (kg m^{-3})
ρ_{air}	Density of air (kg m^{-3})
ρ_{water}	Density of water (kg m^{-3})
ω	Wave circular frequency (rad s^{-1})

1. INTRODUCTION

In recent years, with the development of offshore engineering, cylindrical floating bodies are constructed everywhere in seas and oceans such as navigation buoys, floating turbine, ocean observation equipment and wave energy converter. Compared with onshore engineering, offshore engineering located in severe marine environment suffer variety random loads such as waves and currents. Under harsh environmental conditions, the cylindrical floating bodies have large motion response, which seriously affects their safety and seakeeping capability, the hydrodynamic interaction between ocean waves and offshore floating bodies becomes more complex. Therefore, systematically studies on the hydrodynamic performance of cylindrical floating body in regular/irregular waves should be necessary, which can provide guidance and proposal for design of cylindrical floating body. Through the last few decades, the hydrodynamic performance of cylindrical floating bodies has been extensively studied by using different approaches including experiments, analytical/theoretical and numerical methods. An extensive review of these methods can be found in documents. In early days, the interactions between waves and floating bodies have been studied by the analytical method and using frequency–domain analyses based on potential flow theories, which may neglect the fluid viscosity, the nonlinear effect of waves and free surface effect. Therefore, it is limited to solve the motion of a floating body of simple shape in small amplitude waves (compared with the floating body). The potential flow theory is powerful and accurate for solving linear problems, but it performs much less well when the motion of floating body and the waves become significantly nonlinear, as it cannot consider the fluid viscosity. Besides, it is not suitable for solving the interactions between floating body and waves when viscous or turbulence effects of fluid is significant. To get around this issue, a large number of models based on the Navier Stokes equations using either the finite difference method or the finite volume method (FVM) have been developed with various interface-capturing techniques such as the Level Set function, the Volume of Fluid and others which can track continuously of the interface between air, waves and floating body. In addition, meshless methods (Ren, 2015) with improved pressure gradient model and boundary treatment techniques were also used for studying the interactions between waves and floating body for 2D simulations. An improved Moving Particle Semi-Implicit (IMPS) method (Zhang, 2017) was introduced and conducted to study the roll of floating body. Coupled SPH-FEM method (Ma, 2020) was applied and used to the interaction between the waves and simple plate. As far as now, the meshless method is improved with techniques for accurate pressure calculation or computational efficiency, which is usually used for analyse the simple shaped body.

The studies of the interactions between waves and floating body have been extensively reported in the literature for a wide range of researches and applications (Betsy, 2014; Juhun, 2016; Tong, 2018; Wang, 2015). The FVM method discretizes the computational domain into a series of structured or unstructured fixed grids and obtains the distribution of physical quantities such as mass, velocity and energy in the computational domain by calculating the flux of mass, momentum and energy across the boundary of the grid element. When the FVM method is used to study the fluid and structure interaction problem, the additional interface identification models are needed to track the free surface flow and deal with the interface of fluid and floating body such as VOF model and Level Set model. In 1981, Hird and Nichols performed the VOF method to describe the interface by the components of individual cell volume fractions (Hird and Nichols, 1981). With the advancement of computational fluid dynamics, the VOF method has become a popular approach to deal with large deformations of the free surface, as well as problems where the motion of solid body are present. Some commercial software such as STARCCM+ or FLUENT and open-source platform for instance OpenFOAM based on VOF method are applied for all this kind simulations. Kristiansen et al. (2005) simulated the diffraction of a large cylinder in a three-dimensional model using the VOF method and compared the CFD calculation results with the PIV experiment results (Kristiansen, 2005). Zhang et al. (2013) used the two-phase flow VOF method to study the interaction between the complex moving rigid structures and nonlinear free surface in engineering (Zhang, 2013). Ashish Pathak and Mehdi Raessi (2016) performed VOF-based solver to study the interaction between two fluids and moving rigid bodies using the fictitious domain method (Ashish and Mehdi, 2016). Islam et al. (2019) used OpenFOAM with the VOF method to study the wave radiation by a box-type floating structure, demonstrating reliability and high fidelity of the model (Islam, 2019). Wang et al. (2020) analysed the characteristic and various components of heave damping of the sandglass-type floating body by using the CFD method (Wang, 2021). Therefore, the two-phase flow VOF method with overset-grid technique is used to consider nonlinear motion of the complex structured floating bodies and large deformation of the free surface for all the numerical simulations in this paper which cannot be considered by the Potential theory.

The paper consists of five parts. After the introduction, the Reynolds Averaged Navier Stokes (RANS) equations and the two phase VOF model are presented in Section 2. The three-dimensional (3D) mesh is constructed in this study. The overset-grid technique is widely used to consider the interaction between fluid and structures, the fluid flow around complex shape bodies and the flow around complex multi-body relative motion. The overlapping mesh technology can break the constraint relationship between cylindrical floating body and mesh, which enable to consider a large six degree of freedom motion of cylindrical floating body on the free surface. The CFD set–up and the computational domain are presented in Section 3. In Section 4, the grid dependent validation is conducted, and the numerical wave tank is also validated against with the analytical results of regular wave, demonstrating reliability and high fidelity of the numerical wave tank. In Section 5, three types of cylindrical floating body with flat damping device, cylindrical damping device and without damping device are performed in the numerical wave tank with the overset grid technology under irregular/regular waves. The damping devices are designed for cylindrical floating bodies to have a short resonance period in pitch and the floating bodies will move in phase with the waves. The displacements, rotations, and accelerations are recorded. The relationships between these motions and the propagating waves are also illustrated. The effects of the damping devices are discussed. Finally, the conclusions of this work are drawn.

2. MATHEMATICAL FORMULATION

2.1 GOVERNING EQUATIONS

The RANS equation is a universal governing equation of kinematics and dynamics of viscous fluid fundamental equation, which is the basic equation to solve the viscous fluid flow field. It can be written as follows:

$$\frac{\partial \rho}{\partial t}+\frac{\partial}{\partial x_i}\left(\rho u_i\right)=0 \tag{1}$$

$$\frac{\partial}{\partial t}\left(\rho u_i\right)+\frac{\partial}{\partial x_j}\left(\rho u_j u_i\right)=-\frac{\partial p}{\partial x_i}+\frac{\partial \sigma_{ij}}{\partial x_j}+\frac{\partial}{\partial x_j}\left(-\rho u_i^{'} u_j^{'}\right) \tag{2}$$

where, u_i, u_j are the time averaged velocity in the direction of x_i and x_j, respectively. $u_i^{'}$ and $u_j^{'}$ are the velocity component pulsation value in the direction of x_i and x_j. t is time; ρ is density of the effective flow; p is pressure field. $\rho u_i^{'} u_j^{'}$ is the Reynolds stress term.

For the turbulence model, an improved RNG k-ε model based on the k-ε two-equation model is applied in this paper, which is a turbulence model suitable for the calculation of complex viscous flow field. The equations are as follows:

The kinetic energy equation of turbulence (k equation) is:

$$\frac{\partial}{\partial t}(\rho k)+\frac{\partial}{\partial x_i}(\rho k u_i)=\frac{\partial}{\partial x_j}\left[\left(\mu+\frac{\mu_t}{\sigma_k}\right)\frac{\partial k}{\partial x_j}\right]+P_k-\rho\varepsilon \tag{3}$$

The Turbulent energy dissipation rate equation (ε equation) is:

$$\begin{aligned}&\frac{\partial}{\partial t}(\rho\varepsilon)+\frac{\partial}{\partial x_i}(\rho\varepsilon u_i)=\\&\frac{\partial}{\partial x_j}\left[\left(\mu+\frac{\mu_t}{\sigma_\varepsilon}\right)\frac{\partial \varepsilon}{\partial x_j}\right]+C_{\varepsilon 1}\frac{\varepsilon}{k}P_k-C_{\varepsilon 2}\rho\frac{\varepsilon^2}{k}-R_\varepsilon\end{aligned} \tag{4}$$

where, turbulent viscosity coefficient is $\mu_t=\rho C_\mu\frac{k^2}{\varepsilon}$, the turbulent kinetic energy generates term is $P_k=\mu_t S^2, S=\sqrt{2S_{ij}S_{ij}}$, the mean strain tensor is $S_{ij}=\frac{1}{2}\left(\frac{\partial u_i}{\partial x_j}+\frac{\partial u_j}{\partial x_i}\right)$, the model specific control $R_\varepsilon=\frac{C_\mu\rho\eta^3(1-\eta/\eta_0)}{1+\beta\eta^3}\frac{\varepsilon^2}{k},\eta=\frac{Sk}{\varepsilon}$; The values of constants in RNG *k*-*ε* model are $\sigma_k=1.39$, $\sigma_\varepsilon=1.39$, $C_{\varepsilon 1}=1.42$, $C_{\varepsilon 2}=1.68$, $C_\mu=0.0845$, $\eta_0=4.38$, $\beta=0.012$.

The Eulerian method named the VOF method is adopted to capture the free surface and the interface. This method is a way to track the evolution of free surface by calculating the volume fraction of water in each grid cell. The equation for the volume fraction is as follow:

$$\frac{\partial\alpha}{\partial t}+\frac{\partial}{\partial x_j}\left(u_j\alpha\right)=0 \tag{5}$$

where *α* represents the volume fraction of water, in contrast 1-*α* represents the volume fraction of air. The volume fraction of each phase is used as the weighting factor of weight function to obtain the mixture properties, for calculating molecule viscosity and the density.

$$\rho=\alpha\rho_{water}+(1-\alpha)\rho_{air} \tag{6}$$

$$\mu=\alpha\mu_{water}+(1-\alpha)\mu_{air} \tag{7}$$

where ρ_{water} and ρ_{air} are the density of water and air, respectively. μ_{water} and μ_{air} are molecule viscosity coefficient of water and air, respectively.

When Eq. (6) and Eq. (7) are substituted into Eq. (1) and Eq. (2), the momentum equation of air-water two-phase flow is calculated for simulation.

2.2 REGULAR AND IRREGULAR WAVE THEORY

The velocity vector of regular wave is specified by Stokes wave in FLUENT solver. The theoretical velocity of second-order Stokes regular wave can be expressed by following equations:

$$\begin{aligned}&\eta=\frac{H}{2}cos(kx-\omega t)\\&+\frac{H^2k}{16}\frac{cosh\,kh}{sinh^3\,kh}(2+cosh\,2kh)cos\,2(kx-\omega t),\end{aligned} \tag{8}$$

$$\begin{aligned}&\varphi=-\frac{Hg}{2\omega}\frac{cosh\,k(h+z)}{cosh\,kh}sin(kx-\omega t)\\&-\frac{3}{32}H^2\omega\frac{cosh\,2k(h+z)}{sinh^4\,kh}sin\,2(kx-\omega t),\end{aligned} \tag{9}$$

$$\begin{aligned}&u=\frac{H}{2}\frac{gk}{\omega}\frac{cosh\,k(h+z)}{cosh\,kh}cos(kx-\omega t)\\&+\frac{3}{16}\frac{H^2\omega k\,cosh\,2k(h+z)}{sinh^4\,kh}cos\,2(kx-\omega t),\end{aligned} \tag{10}$$

$$\begin{aligned}&w=\frac{H}{2}\frac{gk}{\omega}\frac{sinh\,k(h+z)}{cosh\,kh}sin(kx-\omega t)\\&+\frac{3}{16}\frac{H^2\omega k\,sinh\,2k(h+z)}{sinh^4\,kh}sin\,2(kx-\omega t),\end{aligned}$$

(11)

$$\omega^2=gk\tanh kh.$$

(12)

where *H*, *k*, *ω* and *h* are wave height, wave number, wave circular frequency and water depth, respectively. *x* is the distance from the origin to the wave-making point.

For the irregular wave simulation, the modified JONSWAP spectrum is chosen as the target spectrum, which can be expressed as follows (Goda &Yoshimi, 1999):

$$S(f)=\beta_j H_{1/3}^2 T_P^{-4} f^{-5} exp\left[-1.25(T_P f)^{-4}\right]\gamma^{exp\left[-(f/f_P-1.0)^2/(2\sigma^2)\right]},$$

(13)

$$\beta_j=\frac{0.06238\times(1.094-0.001915\,ln\,\gamma)}{0.23+0.0336\gamma-0.185\times(1.9+\gamma)^{-1}},$$

(14)

$$T_p=\frac{T_{1/3}}{1.0-0.132(\gamma+0.2)^{-0.559}},$$

(15)

$$\sigma=\begin{cases}0.07 & f\le f_P\\0.09 & f>f_P\end{cases}$$

where $H_{1/3}$ and $T_{1/3}$ are the significant wave height and period, respectively. f is the frequency. γ is the peak enhancement factor, $\gamma = 3.3$. T_P and f_P denote the wave period and the frequency at the spectral peak, respectively.

3. CFD SET-UP

3.1 GEOMETRIC PARAMETERS OF THE DEVICE

The full-scale models of three cylindrical floating bodies with flat damping device, cylindrical damping device and without damping device are performed in this section. They are all composed with pontoon, equipment cabin, counterweight, spar and different damping devices. Figure 1 shows the geometric model diagram of three cylindrical floating bodies with flat damping device, cylindrical damping device and without damping device, the physical parameters of three cylindrical floating bodies are described in Table 1.

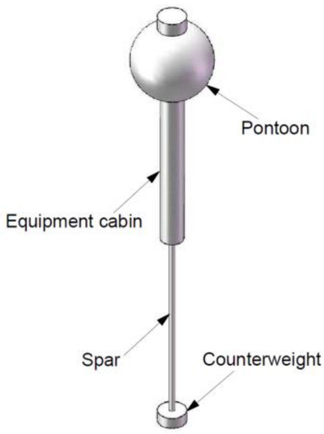

(a) Without damping device floating body

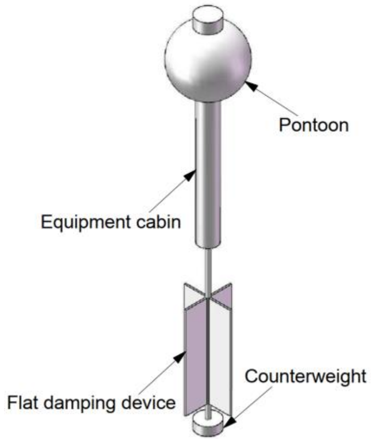

(b) Flat damping device floating body

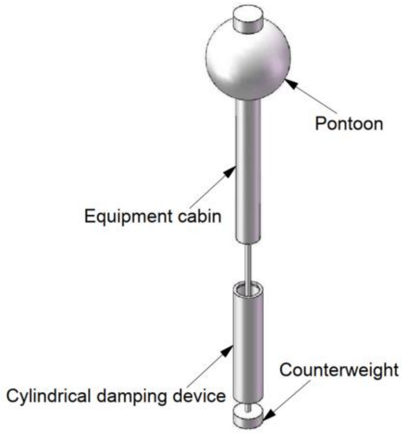

(c) Cylindrical damping device floating body

Figure 1: Geometric model diagram of three cylindrical floating bodies

Table 1 Principal dimensions of three cylindrical floating bodies

Principal dimensions	Without damping device floating body	Flat damping device floating body	Cylindrical damping device floating body
Weight/*kg*	37.30	40.79	40.30
Designed water line /*m*	1.70	1.87	1.80
Height /*m*	2.50	2.50	2.50
Diameter /*m*	0.40	0.40	0.4
Rolling inertia moment/$kg \times m^2$	29.49	31.36	30.99
Pitching inertia moment /$kg \times m^2$	29.49	31.36	30.99
Yawing inertia moment/$kg \times m^2$	0.124	0.144	0.14

3.2 CALCULATION DOMAIN

The CFD model used in this study assumes incompressible fluid in the NWT considering that air compressibility effect is negligible in the full scale model. The flow motion of the incompressible fluid are described by the continuity and RANS equations. The Volume of Fluid (VOF) method is used to model and track the free surface motion. All simulations are conducted using the RANS–VOF solver in FLUENT which uses the finite volume method to discretise the integral formulation of the RANS equations described in section 2. The computational fluid domain with the assigned boundary conditions are presented in Figure 2a. To ensure a high accuracy and high efficiency, different domain sizes are tested to find a reasonable domain size for reasonable computational resources. The size of background region is established with 36H×12.5D×8.8H, overset region is established with 2.24H×5.0D×5.0D around the cylindrical floating body（see Figure 2）. The H and D are the height and diameter of the cylindrical floating body separately. The damping zone of length 2L is placed at the end of the NWT for eliminating waves, L means the wavelength. Waves are damped by adding a resistance term to the equation for the vertical velocity component in the damping zone. Which is recommended at least one wavelength for the damping zone; however, it is found to be insufficient for accommodating and damping radiated waves from the model motion. A damping zone of length 2L is selected to be adequate, so 2L is used in this calculation. The width of the NWT is set as 12.5 diameter of the cylindrical floating body with a symmetry plane. Considering the symmetry of the cylindrical floating body, the assumption of using a symmetry plane is appropriate. The symmetry boundary is used for the bottom of tank and the water depth is set to 50*m*. Tank side is defined as slip wall, while a hydrostatic wave pressure is defined at the top and outlet boundaries. A summary of the numerical settings and the initial conditions (showing in Figure 2) used herein can be found in Ref. (Elhanafi, 2017). In case that the dimensions of the three types of cylindrical floating bodies are similar, the calculation domain of three types of cylindrical floating bodies are the same in the CFD simulations.

To accurately capture the deformation of the VOF free surface, the refinement meshes are set up in both air-water interface, and the background region meshes near the overset region are also encrypted.

The overset technology is used in the whole simulations. Two different regions are created in the computational domain: a background region representing the NWT and a separate overset region which covers the cylindrical floating body model. Between the background and overset regions, an overset interface is created. As the overset region moves with the cylindrical floating body, the overlapping area changes, and flow information exchanges between both regions via a linear interpolation method. In order to obtain good data transmission and numerical exchange, the mesh size on the overlapping area should set to be the same magnitude.

The natural periods of the cylindrical floating body in surge, heave and pitch, which are the dominant degrees of freedom of affecting the device stability under waves in this study, therefore 3DOF model are used to capture the motion of the cylindrical floating body. The user define file is used to specify the mass, moment of inertia, and release the floating body three kind motions: pitch, heave and surge. Figure 3 displays the 3DOF motion solution process.

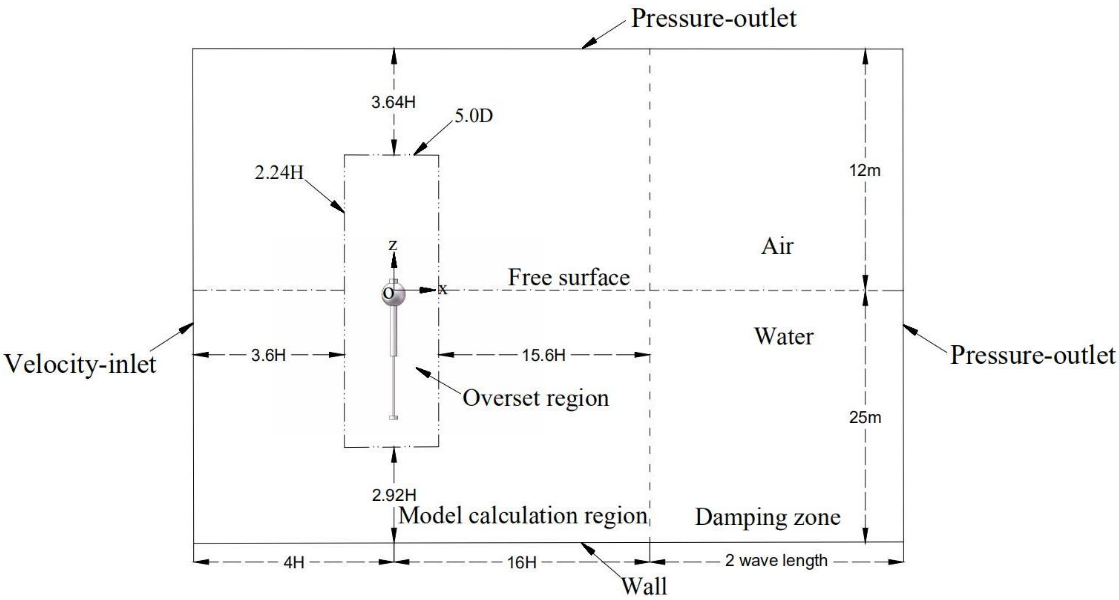

Figure 2: Computational fluid domain (not to scale)

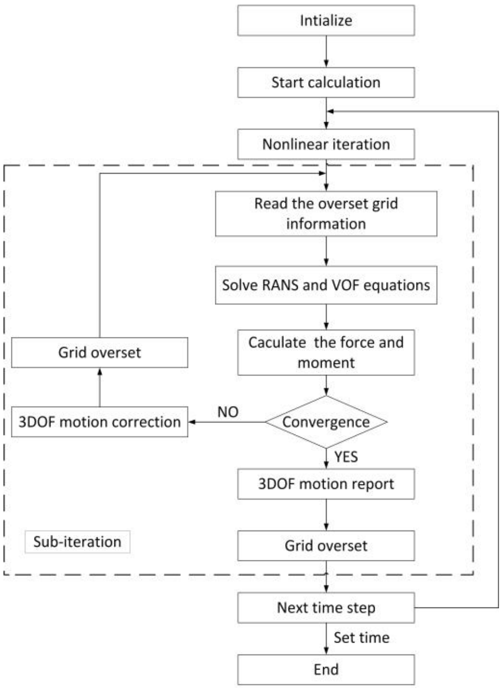

Figure 3: The solution process of the numerical calculation

4. CFD VALIDATION

4.1 THE GRID DEPENDENT VALIDATION

The cylindrical floating body with cylindrical damping device is used as the calculation object for grid dependent validation. Three numbers of grid models are established separately 2.4 million, 3.3 million and 4.5 million which increases in $\sqrt{2}$ times. The grid size of overset region for three kind of grid models are 0.015m, 0.01m and 0.005m, respectively. The regular wave with wave period 3*s* and wave height 0.27*m* are set up for this CFD calculations. The pitch motion of cylindrical floating body is selected as the dominant degree of freedom of affecting the device stability. The CFD calculation results are summarized in Figure 4. It can be seen that there is no large differences between the results of 3.3 million and 4.5 million calculation with the extension of calculation time. Thus, the mesh model of 3.3 million is chosen for the whole numerical simulations in account of the calculation efficiency and accuracy.

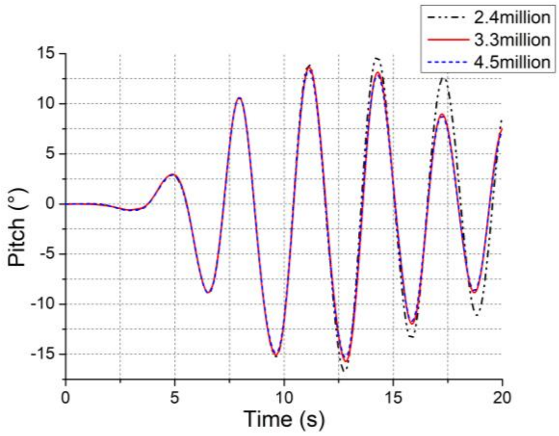

Figure 4: The calculation results for mesh dependence validation

4.2 NUMERICAL WAVE VALIDATION

The regular wave with wave period 2.5s and wave height 0.19m is performed for validation of numerical wave. The calculation domain is the same as Figure 2 without the cylindrical floating body model. The results from the linear wave theory for regular waves are utilized in this section to validate the constructed 3D CFD model described in Section 3. Figure 5 illustrates the results of the wave propagation at t=30s which is measured by the volume fraction of water on the free surface. The comparisons between CFD and analytical results for incident wave elevation, the CFD result is closed to the analytical result with errors of less than 5%. Figure 6 shows the time history of regular wave at x=5m from the inlet boundary. The CFD result is also in good agreement with the analytical result, it is concluded that the numerical wave tank established in this simulation can generate long time and stable wave for the following numerical simulations.

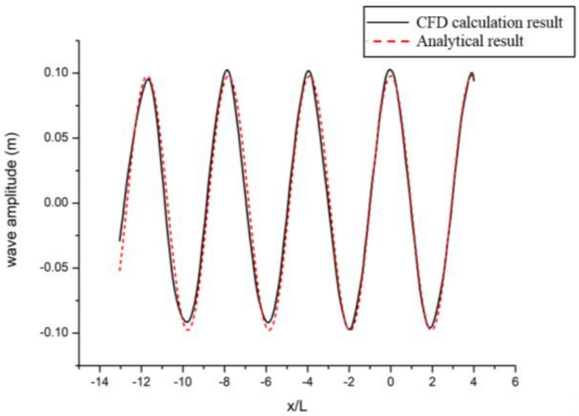

Figure 5: Wave propagation at t=30s

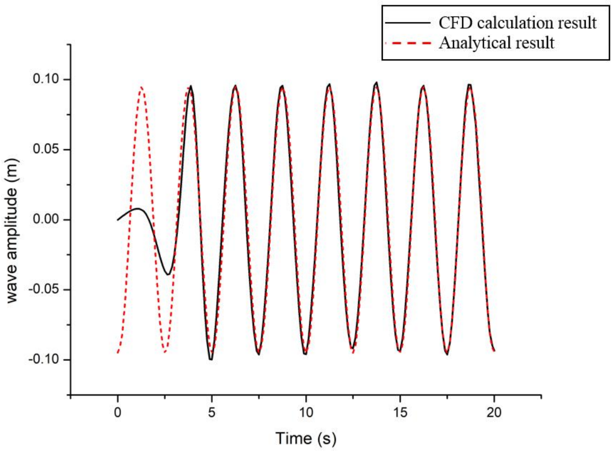

Figure 6: The time history of regular wave at x=5m from the inlet boundary

5. RESULTS AND DISCUSSION

5.1 THE SIMULATIONS IN REGULAR WAVE

The floating body equipped with cylindrical damping device in regular waves are simulated and discussed in this section. The calculation domain is the same as section 4. The wave parameters of regular wave conditions are listed in Table 2.

Table 2 Regular wave parameters

Regular wave cases	Wave height	Wave length	Wave period
Case 1	0.12*m*	6.24*m*	2.00*s*
Case 2	0.19*m*	9.76*m*	2.50*s*
Case 3	0.27*m*	14.05*m*	3.00*s*
Case 4	0.37*m*	19.13*m*	3.50*s*
Case 5	0.37*m*	24.98*m*	4.00*s*
Case 6	0.37*m*	39.00*m*	5.00*s*

Figure 7 shows the time history of pitch motion in regular wave cases 1~6. The pitch motion of the cylindrical floating body is described in Table 3 including maximum pitch angle, period of pitch motion and averaged pitch angle after fast Fourier transform (FFT). Compared with the maximum pitch angle and averaged pitch angle in regular wave cases 1~6, the pitch motion of the cylindrical floating body is affected by the wave height and period in significant measure. When the wave period is short and wave height is large, the pitch motion of cylindrical floating body with cylindrical damping devices is violent. When the wave height is the same in regular wave cases 4~6, the pitch motion begins to slow down with increasing wave period. When the pitch motion of cylindrical floating body is gentle, the pitch period of floating body is closed to the wave period of regular wave. On the contrary, when the pitch motion is violent, there are large differences between the pitch period of the floating body and the wave period.

Table 3 Pitch motion response

Regular wave	Maximum pitch angle		Period of pitch motion	Averaged pitch angle
	Anti-clockwise	Clockwise		
Case 1	3.95°	-3.28°	2.08*s*	1.45°
Case 2	5.13°	-8.53°	2.50*s*	3.68°
Case 3	13.61°	-15.70°	2.86*s*	10.13°
Case 4	22.55°	-26.66°	3.36*s*	17.79°
Case 5	19.38°	-20.10°	3.75*s*	15.33°
Case 6	8.13°	-8.44°	5.00*s*	3.37°

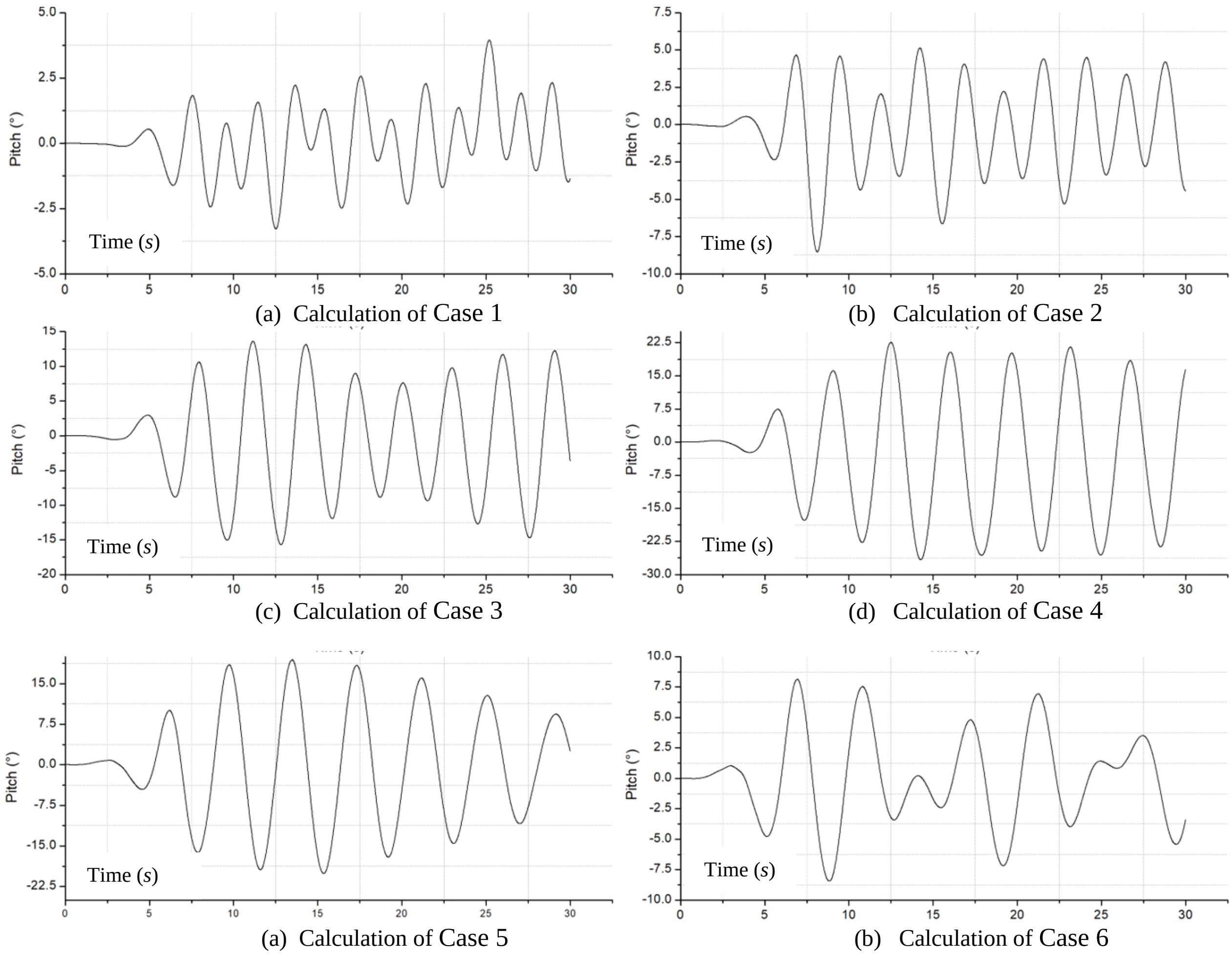

Figure 7: The time history of pitch motion of the cylindrical floating body with cylindrical damping devices

Meanwhile, the time history of heave motion of the cylindrical floating body in regular wave cases 1~6 are illustrated in Figure 8. The maximum heave motion and the period of heave motion are listed in Table 4. In accordance with the results of pitch motion, the cylindrical floating body with cylindrical damping devices turn up violent heave motion in regular wave with short wave period and large wave height. When the wave height is constant in regular wave cases 4~6, the heave motion of the floating body with cylindrical damping devices slow down with the increasing wave period.

Table 4 Heave motion response

Regular wave	Maximum Heave motion		Period of heave motion
	Sink	Rise	
Case 1	-0.067*m*	0.031*m*	2.50*s*
Case 2	-0.197*m*	0.092*m*	2.50*s*
Case 3	-0.258*m*	0.196*m*	2.86*s*
Case 4	-0.367*m*	0.325*m*	3.75*s*
Case 5	-0.241*m*	0.219*m*	4.17*s*
Case 6	-0.177*m*	0.190*m*	5.00*s*

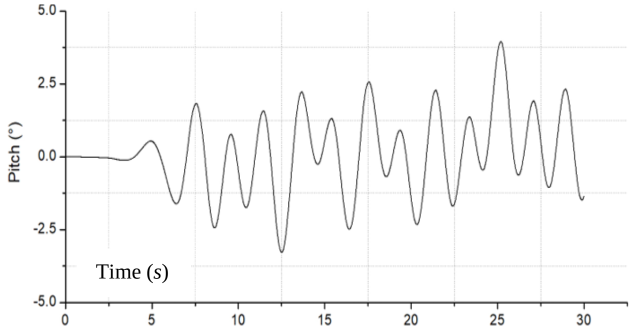

(a) Calculation of Case 1

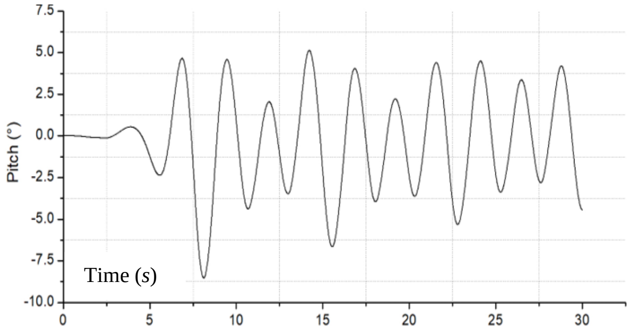

(b) Calculation of Case 2

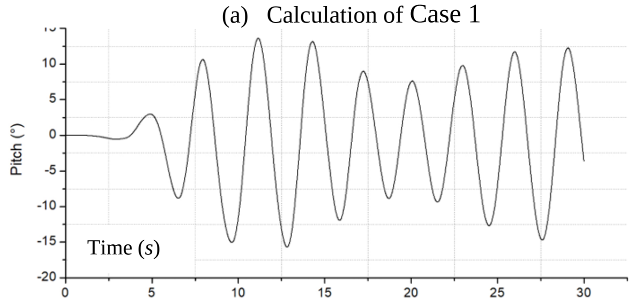

(c) Calculation of Case 3

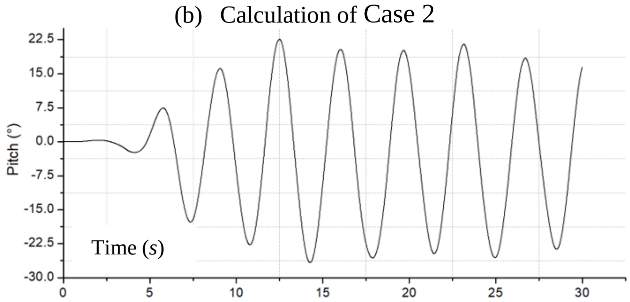

(d) Calculation of Case 4

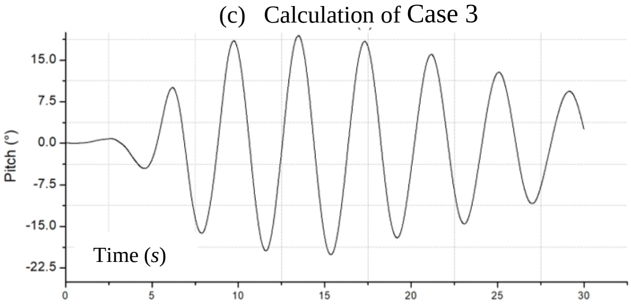

(e) Calculation of Case 5

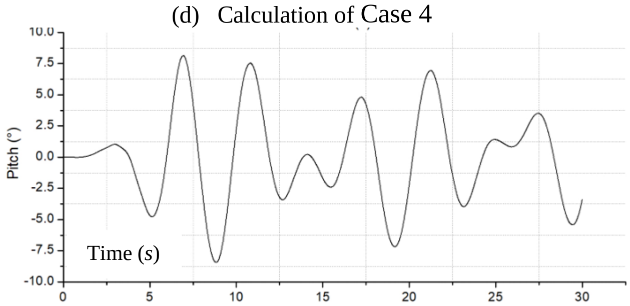

(f) Calculation of Case 6

Figure 8: The time history of heave motion of the cylindrical floating body

5.2 THE SIMULATIONS IN IRREGULAR WAVE

For further study, the results in this section are limited to irregular wave with the parameters wave height=1.84m, peak spectral period=6.00s, period range=3.42~9.02s. The irregular wave is generated by applying JONSWAP wave spectrum in the FLUENT solver. The floating body equipped without damping device, with flat damping device and cylindrical damping device in irregular waves are simulated. The time history of irregular wave heights are shown in Figure 9.

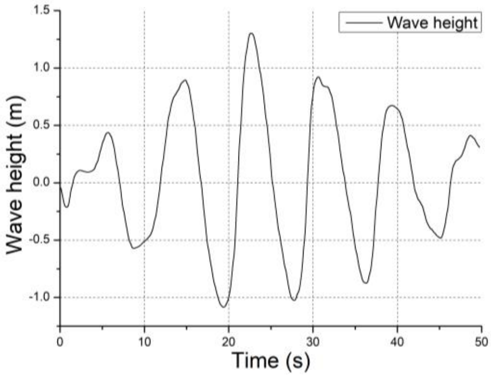

(a) The CFD calculation of floating body without damping device

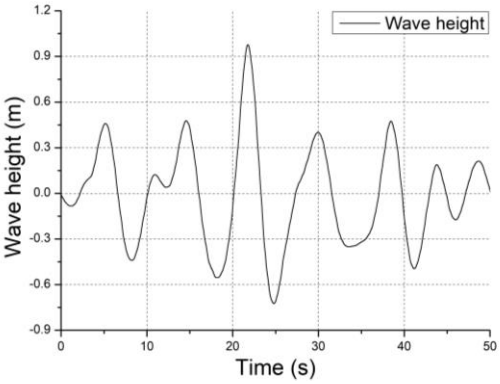

(b) The CFD calculation of floating body with flat damping device

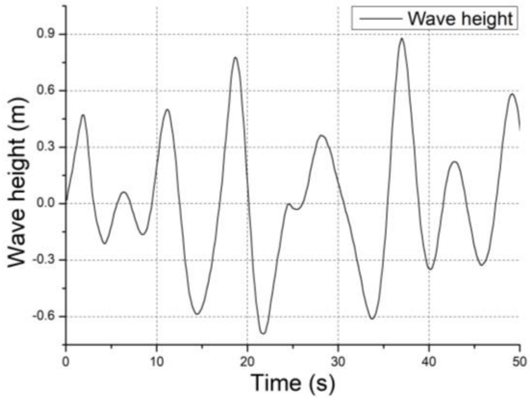

(c) The CFD calculation of floating body with cylindrical damping device

Figure 9: The time history of irregular wave heights in three CFD calculations

The hydrodynamic performance of the three cylindrical floating bodies with different devices are compared in Figure 10. The pitch motion of the three type cylindrical floating bodies in irregular waves are described in figures. The maximum pitch angle, pitch frequency and averaged pitch angle after FFT are listed in Table 7. It can be seen that the pitch motion of the cylindrical floating body without damping device is very intense than others, after installing the damping device, the pitch motion of the cylindrical floating body decreases obviously. The damping device not only reduces the maximum pitch angle, but also reduces the averaged pitch angle and pitch frequency. By comparing with the results of two damping devices, the flat damping device has a better effect in seakeeping ability. This figures show the importance of damping devices that can be utilized to tune the motion of the cylindrical floating body. Table 8 and 9 respectively show the velocity and acceleration of pitch motion. When the cylindrical floating body without damping device, the cylindrical floating body will have large pitch velocity and pitch acceleration, after installing the damping device, the pitching velocity and acceleration decrease apparently, and the effect of flat damping device is better than that of cylindrical damping device.

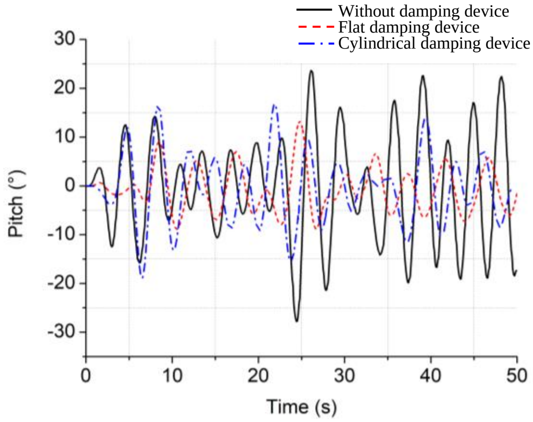

Figure 10: Pitch motion of the cylindrical floating body with three type damping devices

Table 7 Cylindrical floating body pitch motion response

Cylindrical floating body	Maximum pitch angle		Frequency of pitch motion	Averaged Pitch angle
	Anticlockwise	Clockwise		
Without damping device	23.7°	-27.8°	0.3Hz	9.6°
Flat damping device	13.2°	-8.9°	0.24Hz	3.96°
Cylindrical damping device	16.8°	-18.9°	0.278Hz	6.5°

Table 8 Cylindrical floating body pitch motion velocity

Cylindrical floating bodies	Maximum pitch velocity		Pitch velocity
	Anti-clockwise	Clockwise	
Without damping device	0.77*rad/s*	-0.67*rad/s*	0.41*rad/s*
Flat damping device	0.27*rad/s*	-0.32*rad/s*	0.10*rad/s*
Cylindrical damping device	0.50*rad/s*	-0.49*rad/s*	0.20*rad/s*

Table 9 Cylindrical floating body pitch motion acceleration

Cylindrical floating bodies	Maximum Pitch acceleration		Pitch acceleration
	Anti-clockwise	Clockwise	
Without damping device	1.27rad/s^2	-1.29rad/s^2	0.74rad/s^2
Flat damping device	0.47rad/s^2	-0.55rad/s^2	0.15rad/s^2
Cylindrical damping device	1.05rad/s^2	-0.89rad/s^2	0.35rad/s^2

The results show that the pitch motion characteristic of the cylindrical floating body is closely related to the damping device and its shape, the flat damping device can reduce the motion response of floating body more effectively than the cylindrical damping device. However, when the flat damping device is subjected to the action of oblique waves, the cylindrical floating body will rotate, which is not benefited to the normal operation of the cylindrical floating body. This problem should be considered in the design of damping device.

6. CONCLUSIONS

This paper investigated the motion characteristics of three cylindrical floating bodies with flat damping device, cylindrical damping device and without damping device in waves by using the VOF method with overset-grid technique. The effect and the shape of damping device on the hydrodynamic performance were discussed. The following conclusions are made:

(1) The damping device can reduce the motion of the cylindrical floating body in waves. It can improve the stability of the cylindrical floating body.

(2) The performance of the damping device is related to the shape. The flat damping device is obviously better than that of the cylindrical damping device in seakeeping ability.

(3) The motion of the cylindrical floating body with cylindrical damping device is related to the wave period and wave height. Under regular wave conditions with short wave period and high wave height, the violent movement occurs.

The results show the Volume of Fluid method with overset-grid technique is suitable for modelling interactions between complex body and waves, and the results may provide guidelines in the motion characteristics analysis and the damping device prototype design in waves.

7. ACKNOWLEDGEMENTS

The authors would like to acknowledge the support of the National Natural Science Foundation of China (No. 51720105011, No. 52071243 and No.52101371) and the Equipment Pre-Research Project (No. 61402070105).

8. REFERENCES

1. ELHANAFI, A., MACFARLANE, G., FLEMING, A., LEONG, Z. (2017) *Scaling and air compressibility effects on a three-dimensional offshore stationary OWC wave energy converter*. Applied Energy. 189:1–20.
2. HIRT, C. W, NICHOLS, B. D. (1981) *Volume of fluid (VOF) method for the dynamics of free boundaries*. Journal of computational physics, 39 (1): 201-225.
3. ISLAM, H., MOHAPATRA, S.C., GADEILO, J., GUEDES SOARES, C. (2019) *OpenFOAM analysis of the wave radiation by a box-type floating structure*. Ocean Engineering. 193:106532.
4. KRISTIANSEN, T., BAARHOLM, R., RORTVEIT, G. J, HANSEN, E. W., STANSBERG, C. T. (2005) *Kinematics in a diffracted wave field: particle image velocimetry (PIV) and numerical models* [C]. In: ASME 2005 24th International Conference on Offshore Mechanics and Arctic Engineering. American Society of Mechanical Engineers Digital Collection. 827-835.
5. MA, C., IIJIMA, K., and OKA, M. (2020) *Nonlinear waves in a floating thin elastic plate, predicted by a coupled SPH and FEM simulation and by an analytical solution*. Ocean Engineering. 204:107243.
6. PATHAK, A., RAESSI, M. (2016) *A 3D, fully Eulerian, VOF-based solver to study the interaction between two fluids and moving rigid bodies using the fictitious domain method*. Journal of Computational Physics. 311: 87-113.
7. REN, B., HE, M., DONG, P., et al. (2015) *Nonlinear simulations of wave-induced motions of a freely floating body using WCSPH method*. Applied Ocean Research. 50:1-12.
8. SEIFFERT, B., HAYATDAVOODI, M., ERTEKIN, R. C. (2014) *Experiments and computations of solitary-wave forces on a coastal-bridge deck. Part I: Flat Plate*. Coastal Engineering. 88:194-209.
9. SONG, J., SO, S., LIM, H. (2016) *Dynamic characteristics between waves and a floating cylindrical body connected to a tension-leg mooring cable placed in a simulated offshore environment*. International Journal of Naval Architecture and Ocean Engineering. 8(4):375-385.
10. TONG, J., LIN, T., SHIH, M., et al. (2018) *An alternative method for computing hydrostatic performances of a floating body with arbitrary geometrical configurations*. Ocean Engineering. 160:301-310.
11. WANG, Y. (2015) *Design of a cylindrical buoy for a wave energy converter*. Ocean Engineering. 160:301-310.
12. WANG, W., RAN, X., ZHAO, Z., HUANG, Y. (2021) *Comparative analysis on various components of heave damping for sandglass-type floating body*. Ocean Engineering. 221(1):108555.
13. YOSHIMI, G. (1999) *A comparative review on the functional forms of directional wave spectrum*. Coastal Engineering. 41 (1): 1-20.
14. ZHANG, Y., and WAN, D. (2017) *Numerical study of interactions between waves and free rolling body by IMPS method*. Computers & Fluids. 155 (20):124-133
15. ZHANG, C., ZHANG, W., LIN, N., TANG, Y., ZHAO, C., GU, J., LIN, W., CHEN, X., QIU, A. (2013) *A two-phase flow model coupling with volume of fluid and immersed boundary methods for free surface and moving structure problems*. Ocean Engineering. 74: 107-124.